

**EJECTA- AND SIZE-SCALING CONSIDERATIONS FROM IMPACTS OF GLASS PROJECTILES INTO SAND.** J.L.B. Anderson<sup>1</sup>, M.J. Cintala<sup>2</sup>, S.A. Siebenaler,<sup>1</sup> and O.S. Barnouin-Jha<sup>3</sup>, <sup>1</sup>Winona State University, Winona, MN (JLAnderson@winona.edu); <sup>2</sup>Code KR, NASA JSC, Houston, TX 77058; <sup>3</sup>Applied Physics Laboratory, The Johns Hopkins University, Laurel, MD 20723.

**Introduction:** One of the most promising means of learning how initial impact conditions are related to the processes leading to the formation of a planetary-scale crater is through scaling relationships.<sup>1,2,3</sup> The first phase of deriving such relationships has led to great insight into the cratering process and has yielded predictive capabilities that are mathematically rigorous and internally consistent. Such derivations typically have treated targets as continuous media; in many, cases, however, planetary materials represent irregular and discontinuous targets, the effects of which on the scaling relationships are still poorly understood.<sup>4,5</sup> We continue to examine the effects of varying impact conditions on the excavation and final dimensions of craters formed in sand. Along with the more commonly treated variables such as impact speed, projectile size and material, and impact angle,<sup>6</sup> such experiments also permit the study of changing granularity and friction angle of the target materials. This contribution presents some of the data collected during and after the impact of glass spheres into a medium-grained sand.

**Data Collection and Experimental Conditions:**

Seven separate impact experiments were performed with the Vertical Impact Facility (VIF) at the Johnson Space Center during which the ejecta were documented with the Ejection-Velocity Measurement System (EVMS).<sup>4</sup> Soda-lime glass spheres with diameters of 3.18 mm were launched at the 0.5-1-mm fraction of a commercial blasting sand at speeds ranging from 0.32 to 1.72 km s<sup>-1</sup>. Because the barrel of the VIF is

fixed, all impacts were normal to the surface of the target. The EVMS produces stroboscopic images of ejecta in flight by flashing a "sheet" of laser light at programmed rates; the illumination sequence initiates at impact, which serves as the reference time for subsequent measurement of particle kinematics. The plane of illumination is normal to the target's surface and passes through the impact point, assuring that fragments of the target with multiple images in the photograph were traveling radially from the impact site (Fig. 1).

**Data:** The velocities of a large number of ejected fragments are measured in each photograph, and those values can be decomposed into their respective speed and launch-angle components. Representative results from one of the shots in this series are illustrated in

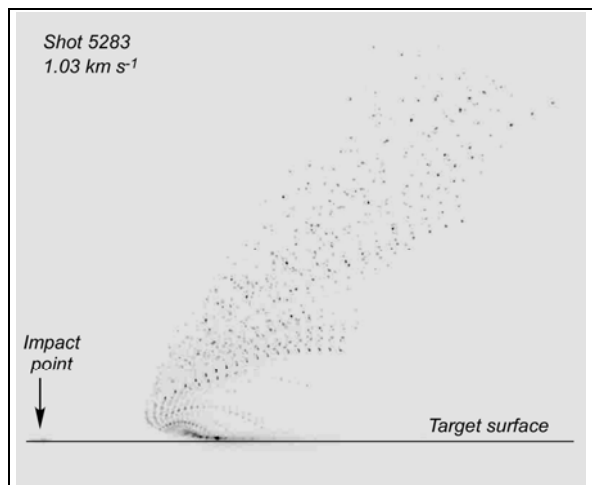


Figure 1. Example of an EVMS photograph of the ejecta from the impact of a 3.18-mm glass sphere into a 0.5-1-mm sand (negative image). Illumination of the ejecta began 15 ms after impact, and continued for 80 ms with a 25- $\mu$ s flash every 4 ms.

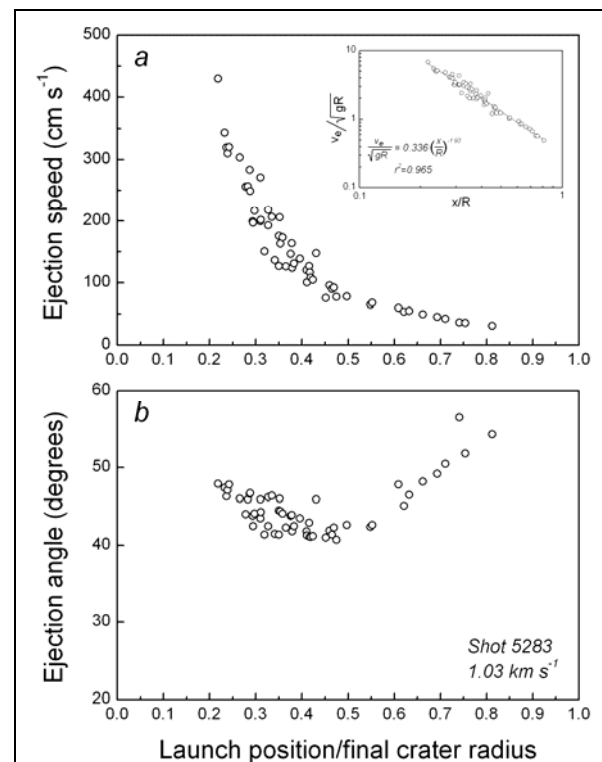


Figure 2. Ejection speeds (a) and angles (b) for fragments measured from the photograph in Fig. 1. Because the illumination did not begin until 15 ms after impact, trajectories with launch positions smaller than about  $0.2R$  were not imaged. The inset in (a) illustrates the results of applying the scaling of [3]. The variables in the equation are as follows:  $x$ , launch position as measured from the impact point;  $R$ , final crater radius;  $v_e$ , ejection speed; and  $g$ , gravitational acceleration. The exponent of the scaled launch position is denoted as  $e_x$ . Note the distinct change in ejection angle with launch position in (b).

Fig. 2. Two different presentations of the data for ejection speed vs. launch position are given, with the inset version representing the scaling procedure of [3]. The impact speed  $U$ , final crater diameter, value of the velocity-scaling scaling exponent, and resulting value of  $\alpha$  (discussed below) for each shot are listed in Table 1.

**Discussion: Ejection-speed scaling.** First-order

Table 1. Data for the seven shots analyzed in this series.

Shot No.	$U$ (km/s)	$D$ (cm)	$e_x$	$\alpha$
5446	0.320	8.10	1.31	0.829
5445	0.548	9.05	2.03	0.593
5443	0.699	9.85	1.86	0.636
5285	0.876	10.20	2.15	0.566
5283	1.031	10.40	1.94	0.615
5286	1.371	11.25	1.47	0.762
5287	1.727	12.00	1.57	0.724

scaling arguments infer that a single parameter  $\alpha$  is related to both the slope of the  $\Pi_R$  vs.  $\Pi_2$  relationship (e.g., Fig. 3) and  $e_x$ .<sup>2,3</sup> Previous experiments, however, yielded a value for  $\alpha$  derived from  $\Pi_R$ - $\Pi_2$  considerations that differed considerably from those determined from  $e_x$ ,<sup>4</sup> a variance that had been attributed to the

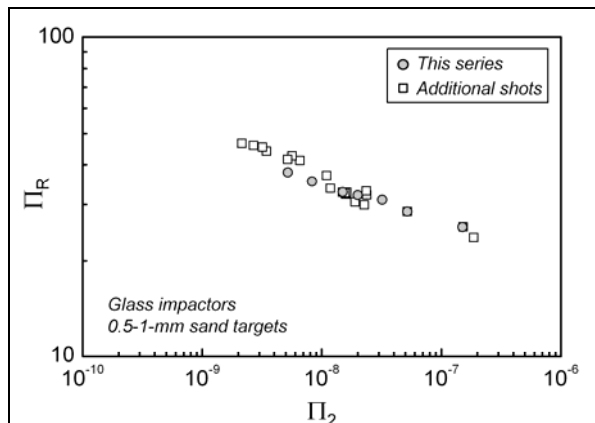


Figure 3. Dimensionless crater radius  $\Pi_R$  as a function of scaled projectile energy  $\Pi_2$  for the seven impacts used in this study as well as for 21 other experiments using 3.18-mm glass projectiles.

coarseness of the sand targets (a mean value of 1.7 mm) relative to the size of the impactors (4.76 mm, giving a ratio  $\gamma$  of 2.7). A fit to the data in Fig. 3 yields a value for  $\alpha$  of 0.453, which is identical to that found for the coarse sand.<sup>4</sup> At the same time, however, the range of  $\alpha$  found from  $e_x$  (Table 1) is very similar to that derived from the coarse-sand experiments.<sup>4</sup> Should these discrepancies in  $\alpha$  be due in fact to the relative grain size of the targets, then the size ratio of the current experiments ( $\gamma=4.5$ ) could still be considered small enough to inhibit "continuum" behavior of the target. It is important to note that separate experiments with larger (6.35-mm) Al impactors in a finer sand (mean grain size of 0.55 mm,  $\gamma=11.5$ )

yielded essentially identical values of  $\alpha$  as determined from the  $\Pi_R$ - $\Pi_2$  slope and  $e_x$ .<sup>7,8</sup> Finally, two of the values for  $\alpha$  as determined from  $e_x$  (Table 1) are above the theoretical maximum value of 0.75. While the value from shot 5286 could be due to uncertainties in the fit, that for shot 5446, the slowest of this series, is well outside the range allowed by the scaling arguments. It is possible that such a low-speed impact into a relatively coarse target violated the point-source assumption of energy release that is the underpinning of many of the scaling arguments.<sup>9</sup> A satisfactory evaluation of this possibility will require additional experiments.

**Ejection angles.** In all seven impacts examined here, the ejection angles are measured to be near  $50^\circ$  above horizontal initially, decreasing slightly as crater growth progresses, to as low as about  $40^\circ$  at scaled launch distances near  $0.5R$ . By the time the crater has achieved 60-70% of its final diameter, ejection angles for all seven impacts are increasing rapidly, approaching  $60^\circ$  at the end of crater growth (Fig. 2b). This evolution of ejection angles as the crater grows has been observed also with aluminum projectiles<sup>4,6</sup> and might be a result of the coupling of energy and momentum from projectile to target, migration of the instantaneous flow-field center below the target's surface,<sup>7</sup> non-proportional crater growth, or internal friction of the target material.

**Conclusions:** The inconsistency in the values of  $\alpha$  determined from the two approaches appears to be an effect of the target material, as impacts into relatively finer-grained targets have consistent values of  $\alpha$ .<sup>7,8</sup> While we have concentrated on grain size here, other material properties that must be addressed are porosity and internal friction. Thickness of the shock front<sup>5</sup> is another factor that could contribute to these results.

These glass and the aluminum<sup>4</sup> impactors possessed densities that were within 10% of each other; the glass invariably shattered upon impact, while the aluminum deformed. The close similarities between the products of the two series imply that complete disruption of the impactor might not be required to produce the same excavation-stage flow.

**References:** <sup>1</sup>Chabai, A.J. (1965) *JGR*, 70, 5075. <sup>2</sup>Holsapple K.A. and Schmidt R.M. (1982) *JGR.*, 87, 1849. <sup>3</sup>Housen *et al.* (1983) *JGR*, 88, 2485. <sup>4</sup>Cintala M.J. *et al.* (1999) *MAPS*, 34, 605. <sup>5</sup>Barnouin-Jha O.S. *et al.* (2002) *LPSC XXXIII*, abstract #1738. <sup>6</sup>Anderson J.L.B. *et al.* (2003) *JGR* 108, doi:10.1029/2003JE002075. <sup>7</sup>Anderson J.L.B. *et al.* (2004) *MAPS*, 39, 303. <sup>8</sup>Anderson J.L.B., unpublished data. <sup>9</sup>Holsapple K.A. (1987) *JGR*, 92, 6350.